

## On the Coordination Sphere Geometry of Trisacetylacetonato Metal(III) Complexes of the First Transition Series Rationalized by Orbital Phase Coupling Effects

T. SCHÖNHERR, M. A. ATANASOV\* and H.-H. SCHMIDTKE

*Institut für Theoretische Chemie der Universität Düsseldorf, Universitätsstrasse 1, D-4000 Düsseldorf 1, F.R.G.*

(Received January 27, 1987)

### Abstract

The directional contribution of  $\pi$ -bonding effects leading to distortions of chelate complexes from higher symmetry is investigated on the basis of orbital phase coupling introduced into the angular overlap model. For first row transition group acetylacetonates the increase of oxygen–oxygen bites compared to closed shell compounds is well explained from calculated bite angles given in terms of angular overlap parameters. These are derived for the chromium and cobalt compounds from trigonal band splittings in the polarized absorption and CD spectra. Phase coupling effects, in these cases, are found to produce larger distortions than possible Jahn–Teller forces active in the ground and the excited states.

### Introduction

The elucidation of the coordination sphere geometry of trisbidentate complexes has been the object of various investigations [1–6]. Attempts to correlate the ‘bite’ oxygen–oxygen atom separation with the M–O distance [3, 5], the chelate bite angle  $\alpha(\text{OMO})$  or with the metal ion radius to charge ratio [1] have been considered to be largely unsatisfactory [7, 8]. Also, explanations which apply an interligand repulsion model [2] considering the charge density distribution in the chelate ring [6] or, in addition, molecular packing in the crystal [3, 6], did not lead to general rules which could properly describe the geometric distortions found for different trisacetylacetonate M(III) complexes [1–8]. Some of these are almost octahedral (Al, Cr), others (Sc, V, Fe) have compressed ( $\alpha < 90^\circ$ ) and one (Co) has a definitely stretched ( $\alpha > 90^\circ$ ) coordination along the trigonal axis of the complex octahedron. On the basis of the X-ray results it has been concluded that ‘the structural details thus depend on complex factors, probably including the role played by unpaired d-electrons in the central metal ion’ [7]. Since we agree

with this opinion we looked into this problem by applying theoretical models (ligand field theory and angular overlap model) which are able to calculate relative stabilities of small distortions due to complex bonding caused by d-orbital interactions with the orbital system of the ligands.

In the following we will show that the equilibrium geometry of the coordination sphere (the chromophore  $\text{MO}_6$ ) of first transition series metal trisacetylacetonates can be well understood in the framework of an angular overlap model (AOM) which considers also the phase coupling of the molecular orbitals on the chelate ligands [15, 16]. This extension of the model leads to nonadditive contributions to the d-orbital energies due to three-center orbital interactions. Since this model is able to explain the large level splittings of the excited states derived from absorption spectroscopy of tris-chelate complexes [17] it should be applicable also for explaining geometric factors of these compounds in the ground state. In cases where AOM parameters can be determined from the experiment the model will furnish also quantitative results. For excited states the low symmetry band splittings will be well reproduced when the X-ray structural results are used as a basis for the calculation. Shortcomings due to the Jahn–Teller effect in the excited state may be possible and are also discussed.

### Evaluation of d-Orbital Contributions

For an investigation of d-orbital participation to the geometric stability of complex molecules the discussion must start from compounds with inert gas electron configurations on the metal ion as reference systems. Due to the isotropic electron distribution on the central ion only high symmetry molecules arrangements are expected from electronic bonding effects. Directional impacts leading to nuclear distortion then arise primarily from steric reasons caused by interligand repulsion and for chelate complexes by factors connected with the rigidity of the ligands. In metal acetylacetonates the ligand molecules are approximately planar and the oxygen–oxygen bites on

\*On leave of absence from the Bulgarian Academy of Science, Sofia, Bulgaria.

TABLE I. X-ray Data for the Metal–Oxygen Distance  $R$ , Oxygen–Oxygen Bite  $b$  and Bite Angle  $\alpha$  of  $M(\text{acac})_3$  Compounds and Angular Contributions  $\Delta\alpha$  due to d-Orbital  $\pi$ -Bonding Derived from ‘Isotropic’ Parameters  $b^*$  and  $\alpha^*$  (see text)

	Al	Sc	V	Cr	Mn <sup>a</sup>	Fe	Co
Experiment							
Reference	3	9	10	11	12	13	14
$R$ (pm)	189.2	207.0	197.9	195.5	198.5	199.2	188.8
$b$ (pm)	271.7	271.6	274.9	279.1	279.1	274.5	281.9
$\alpha$ (°)	91.8	82.0	88.0	91.1	89.6	87.1	96.6
Theory							
$b^*$ (pm)	← 271.7 for all assumed →						
$\alpha^*$ (°)			86.6	88.0	86.4	86.0	92.0
$\Delta\alpha = \alpha - \alpha^*$			1.4	3.1	3.2	1.1	4.6
$\Delta\alpha$ (calc.) <sup>b</sup>			>0	3.2		>0	3.9

<sup>a</sup>Ground state Jahn–Teller distortion involved. <sup>b</sup>Distortion due to  $p_\pi$ – $d_\pi$  interaction calculated from eqn. (10).

threefold charged metal ions with no d-electrons are almost identical, *i.e.*  $b = 2.716(7)$  for Al(III) and Sc(III), although the metal–oxygen atomic distances  $R$  and bite angles  $\alpha$  are different (see Table I). We conclude that any deviation from this ‘isotropic’ bite  $b^*$  in transition group ions should be attributed to d-orbital contributions distorting the nuclear frameworks due to the anisotropy of  $\pi$ -bonding. With this bite  $b^*$ , assumed to be unchanged for all ions of the first transition series, a hypothetical bite angle  $\alpha^*$  is calculated from the geometric relation

$$\sin(\alpha^*/2) = \frac{b^*}{2R^*} \quad (1)$$

which for the relaxed metal–ligand distance  $R^*$  furnishes the correct bite angle in the case where metal–ligand  $\pi$ -interaction would be neglected. However, since we expect a larger change of the bond energy with respect to  $R$  compared to variation with  $\alpha$ , *i.e.*

$$\frac{\partial E(R, \alpha)}{\partial R} > \frac{\partial E(R, \alpha)}{\partial \alpha} \quad (2)$$

(which is better fulfilled for strong  $\pi$ -bonding) the change in  $R$  due to neglect of d-orbital bond participation is relatively small for a given energy alteration but much larger for  $\alpha$ . We therefore can identify  $R^*$  with the experimental  $R$  in eqn. (1) and consider only changes in the bite angle due to d-orbital contributions. In an  $\alpha$  to  $R$  plot (Fig. 1) we therefore go only by vertical steps when relating the geometrical factors of transition group ions to the line traced by the inert gas ions Al–Sc. Any changes of the oxygen–oxygen bite due to anisotropic bond effects in the chromophore are then reflected only by a change in the bite angle  $\Delta\alpha = \alpha - \alpha^*$  compared to the experimental values  $\alpha$ . The corresponding  $\Delta\alpha$  values are listed in Table I.

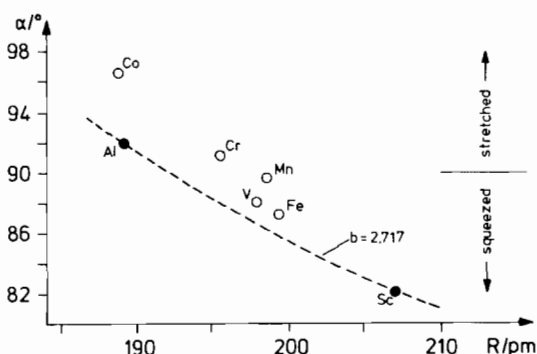


Fig. 1. Bite angle to metal–ligand distance plot from X-ray data of metal trisacetylacetonates. The dashed line illustrates the  $\alpha(R)$  dependence of eqn. (1) for constant oxygen–oxygen bite  $b = 271.7$  pm.

### Angular Overlap Calculations

We concentrate on energy changes and excited state band splittings due to low symmetry distortions using different versions of the AOM in the calculation. Since the ligands contain a planar  $\pi$ -electron system the parameters for  $d_\pi$ – $p_\pi$  interaction are chosen differently for in plane  $e_{\pi\parallel} \equiv e_{\pi c}$  and out of plane  $e_{\pi\perp} \equiv e_{\pi s}$  antibonding. In this model the ligand contributions to the metal orbital energies are still additive. The phase coupling (non-additive) model distinguishes between two out of plane  $\pi$ -parameters, one ( $e_{\pi s}$ ) for in phase coupling and another ( $e'_{\pi s}$ ) for out of phase coupling [17]. The former mechanism applies if the coefficients of atomic orbitals on the ligating atoms in the ligand orbital have an equal sign; out of phase coupling is effective when these coefficients have a different sign. In Table II the AOM perturbation matrix elements are listed for the particular geometry of three planar bidentate ligands of bite angles  $\alpha$  which are mutually perpendicular to each other. For acetylacetonate

TABLE II. Non-vanishing AOM Matrix Elements ( $d_i|V(D_3)|d_j$ ) of d-Orbitals in Trigonally Distorted Bidentate Complexes with Mutually Perpendicular Planar Rings Depending on the Bite Angle  $\alpha$ 

Matrix elements	Additive model	Non-additive model
$(xz xz) = (yz yz) = (xy xy)$	$\frac{3}{2}e_\sigma \cos^2 \alpha + 2e_{\pi s} + 2e_{\pi c} \sin^2 \alpha$	$\left\{ \begin{array}{l} \frac{3}{2}e_\sigma \cos^2 \alpha + 2e_{\pi s} \cos^2(\alpha/2) \\ + 2e'_{\pi s} \sin^2(\alpha/2) + 2e_{\pi c} \sin^2 \alpha \end{array} \right.$
$(xz yz) = (xz xy) = -(yz xy)$	$e_{\pi s} \cos \alpha$	$e_{\pi s} \cos^2(\alpha/2) - e'_{\pi s} \sin^2(\alpha/2)$
$(z^2 z^2) = (x^2 - y^2 x^2 - y^2)$	$\frac{3}{4}e_\sigma(1 + 3 \sin^2 \alpha) + 3e_{\pi c} \cos^2 \alpha$	
$(xy z^2)$	$-\frac{\sqrt{3}}{2}e_\sigma \cos \alpha$	
$(xz z^2) = -(yz z^2)$	$-\frac{\sqrt{3}}{4}e_\sigma \cos \alpha$	
$(xz x^2 - y^2) = (yz x^2 - y^2)$	$-\frac{3}{4}e_\sigma \cos \alpha$	

ligands out of phase interaction can, however, be neglected, *i.e.*  $e'_{\pi s} = 0$ , since the corresponding molecular orbital  $\pi_2$  is much lower in energy than the highest occupied orbital  $\pi_3$  which is the only donor orbital of this ligand [17].

We start by calculating the band splittings of the first spin allowed transitions of Cr- and Co-trisacetylacetonates. The corresponding octahedral states are  ${}^4T_{2g}(t_{2g}^3)$  and  ${}^1T_{1g}(t_{2g}^6)$  which split under  $D_3$  symmetry into  ${}^4A_1$ ,  ${}^4E$  and  ${}^1A_2$ ,  ${}^1E$ , respectively. Neglecting configuration interaction with higher states (which is small, *vide infra*) the AOM expressions for these level differences are obtained from symmetry adapted more-electron functions [18] and can be written in analytical form

$$\Delta E(E - A) = \frac{3}{2} e_{\pi s} \cos \alpha \quad \text{additive model}$$

$$\Delta E(E - A) = \frac{3}{2} [e_{\pi s} \cos^2(\alpha/2) - e'_{\pi s} \sin^2(\alpha/2)] \quad \text{non-additive model} \quad (3)$$

Since the experimental band splitting derived from the measured  $\sigma$ - and  $\pi$ -polarizations is 750–910  $\text{cm}^{-1}$  with the energy level order  $E > A$  for both compounds [19–22], it is immediately seen that only the non-additive model (with vanishing out of phase coupling, *i.e.*  $e'_{\pi s} = 0$ ) is able to reproduce the correct level sequence for experimental bite angles  $\alpha > 90^\circ$  (Table I). This agrees with earlier findings according to which only the phase coupling model is able to account for a correct AOM description of absorption spectra [17].

With respect to the ground state, the bite angle dependence of the total energy of a  $t_{2g}^n$  system with

$n = 1, 2$  or 3 electrons, in the same approximation neglecting off-diagonals to  $e_g$ -orbitals in the perturbation matrix of Table II and setting  $e'_{\pi s} = 0$ , is calculated

$$E(\alpha) = \frac{3}{2} n e_\sigma \cos^2 \alpha + (3n - 3) e_{\pi s} \cos^2(\alpha/2) + 2n e_{\pi c} \sin^2 \alpha + E(n, B, C) \quad (4)$$

the last term denoting the repulsion of the d-electrons given in terms of the Racah parameters  $B$  and  $C$ . This energy is minimal with respect to variation of  $\alpha$  for

$$\cos \alpha = -\frac{3(n-1)}{2n} e_{\pi s} / (3e_\sigma - 4e_{\pi c}) \quad (5)$$

The last contribution in eqn. (4) disappears on differentiation due to the spherical character maintained for the electron repulsion terms. Since  $3e_\sigma - 4e_{\pi c}$  must be positive ( $\sigma$ -bonding is larger than corresponding  $\pi$ -bonding) as is the case for  $e_{\pi s}$  (donor ligands), the bite angle for minimal d-electron energy from eqn. (5) is  $\alpha = 90^\circ$  for  $n = 1$  and  $\alpha > 90^\circ$  for  $n = 2$  or 3. Taking the  $t_{2g} - e_g$  configuration into account leads to potential minima slightly shifted (by about one degree) to higher  $\alpha$ -angles (*vide infra*).

It is noted that the corresponding calculation based on the additive model supplies different results. The ground state energy of a  $t_{2g}^n$  system ( $n = 1, 2$  or 3) using the matrix elements of Table II for this model is

$$E(\alpha) = \frac{3}{2} n e_\sigma \cos^2 \alpha + 2n e_{\pi s} + (n - 3) e_{\pi s} \cos \alpha + 2n e_{\pi c} \sin^2 \alpha + E(n, B, C) \quad (6)$$

which by variation of  $\alpha$  is minimal for

$$\cos \alpha = \left( \frac{3-n}{n} \right) e_{\pi s} / (3e_{\sigma} - 4e_{\pi c}) \quad (7)$$

Since this expression is positive (for  $n = 1$  or  $2$ ) or vanishing ( $n = 3$ ), the bite angle would be  $\alpha \leq 90^\circ$  indicating either a decrease compared to the 'isotropic' bite angle or no distortion at all as a result of  $\pi$ -bonding effects. This is, however, in contrast to the experimental findings (*cf.* Table I). As has been concluded from spectroscopic arguments we therefore note that only the non-additive model which considers phase coupling is able to explain the experimental reality.

For the corresponding low spin Co(III) compound ( $n = 6$ ) the optimal bite angle can be also calculated from eqn. (5) when setting  $n = 3$ , since the energy stabilization for a closed sub-shell configuration ( $n = 6$ ) depends only on diagonal elements of perturbation matrix (Table II) as in the case of a half filled shell ( $n = 3$ ) with singly occupied orbitals. The remaining acetylacetonates listed in Table I, *i.e.* Mn(III) and Fe(III), are high spin complexes with  $t_{2g}^3 e_g$  and  $t_{2g}^3 e_g^2$  configurations, respectively. Their  $\pi$ -electron contribution to low symmetry distortion due to phase coupling is also given by eqn. (5), however, since their  $\sigma$ -contributions arising from diagonal elements (*cf.* Table II) are important, larger deviations from high symmetry are expected yielding trigonal distortions which in part are compensated by restoring forces due to the ligand–ligand repulsion. Since these cannot be described by the present theory without further assumptions, we shall not consider these systems. We may, however, add that occupation of  $e_g$  orbitals increases the tendency towards larger distortions to trigonal symmetry. For Mn(acac)<sub>3</sub> the situation is even more complicated by the presence of a tetragonal Jahn–Teller activity in the ground state [12, 23].

### Quantitative Considerations

The calculation of actual bite angle changes which are governed by phase coupled ligand  $\pi$ -bonding effects are carried out using eqn. (5). The necessary AOM parameters can be obtained from electronic spectra exhibiting low symmetry band splittings which are properly assigned to trigonal level components, *e.g.*, by using polarized spectra. However, only for Cr- and Co-trisacetylacetonate has the trigonal splitting  $\Delta E$  of the first spin allowed transition in octahedral symmetry been determined [19–22]. Corresponding band peaks obtained from circular dichroism spectra [22] are compiled in Table III. The measured band splittings may be related to the energy difference, eqn. (3), of the low symmetry

TABLE III. Band Components (in  $\text{cm}^{-1}$ ) Arising from Trigonal Splitting of First Spin Allowed Transitions Obtained from Circular Dichroism Spectra [22]

	Cr(acac) <sub>3</sub>			Co(acac) <sub>3</sub>				
$\pi$	17650	${}^4A_1$	}	${}^4T_{2g}$	16240	${}^1A_2$	}	${}^1T_{1g}$
$\sigma$	18400	${}^4E$			17150	${}^1E$		
$\Delta E$	750				910			

level components calculated from the non-additive model. Neglecting again out-of-phase coupling, *i.e.*  $e'_{\pi s} = 0$ , this splitting is

$$\Delta E(E - A) = \frac{3}{2} e_{\pi s} \cos^2(\alpha/2) \quad (8)$$

Comparison with eqn. (5) for  $n = 3$  and using the trigonometrical relation  $\cos^2(\alpha/2) = \frac{1}{2}(1 + \cos \alpha)$  yields

$$\Delta E = \frac{3}{4} e_{\pi s} \left( 1 - \frac{e_{\pi s}}{3e_{\sigma} - 4e_{\pi c}} \right) \quad (9)$$

Due to the size of the denominator which is larger than the cubic ligand field parameter  $10Dq = 3e_{\sigma} - 2e_{\pi c} - 2e_{\pi s}$  ( $e_{\pi c} < e_{\pi s}$ ) the second term in eqn. (9) is rather small, *i.e.* with the splitting  $\Delta E = 910 \text{ cm}^{-1}$  measured for the Co compound,  $e_{\pi s}$  must be larger than  $1200 \text{ cm}^{-1}$ . With the reasonable parameter value  $Dq = 1800 \text{ cm}^{-1}$  [24] in the denominator of eqn. (9),  $e_{\pi s}$  is calculated approximately  $1300 \text{ cm}^{-1}$ . The inclusion of  ${}^1E({}^1T_{1g})$  level interaction with the higher  ${}^1E({}^1T_{2g})$  would further increase this value by a limited amount. Insertion of  $e_{\pi s} = 1300 \text{ cm}^{-1}$  and  $\Delta E = 910 \text{ cm}^{-1}$  into eqn. (8) leads to a bite angle of  $\alpha = 93.8^\circ$  resulting in a correction of this angle due to phase coupling effects of  $\Delta\alpha = 3.8^\circ$  which compares well with that derived from the experiment (*cf.* Table I). However, since the determination of the bite angle from eqn. (8) is rather sensitive with respect to a variation of  $\Delta E$  which possibly cannot be determined with the proper precision from the spectra, one should preferably use eqn. (5) in which the ligand field parameter  $10Dq = 3e_{\sigma} - 2e_{\pi c} - 2e_{\pi s}$  which is known with a higher accuracy is introduced

$$\cos \alpha = - \frac{e_{\pi s}}{10Dq + 2e_{\pi s} - 2e_{\pi c}} \quad (10)$$

The plot in Fig. 2 further shows that, with this equation,  $\alpha$  is much less submitted to an uncertainty of  $Dq$  than is eqn. (8) with respect to  $\Delta E$  measurements. In either case  $e_{\pi c}$  is approximated by  $e_{\pi c} = 0.6 e_{\pi s}$  using overlap considerations [25]. The bite angle calculated from eqn. (10) with  $Dq = 1800 \text{ cm}^{-1}$  is  $\alpha = 93.9^\circ$  which agrees with the value obtained from eqn. (8) better than expected. With this angle of  $\alpha$

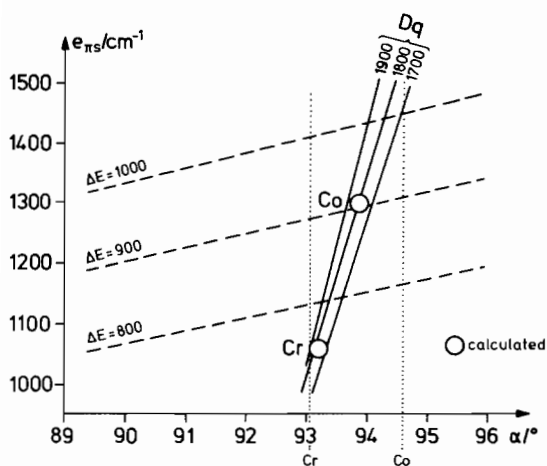


Fig. 2. Dependences of the bite angle  $\alpha$  on the energy splitting  $\Delta E$ , eqn. (8), and the cubic ligand field parameter  $Dq$ , eqn. (10). The  $90^\circ + \Delta\alpha$  values of Table I for Cr and Co are marked as well.

and the hereby confirmed value of  $e_{\pi s} = 1300 \text{ cm}^{-1}$  the other parameter are calculated by the use of eqn. (5) and eqn. (10) to  $e_\sigma = 7580 \text{ cm}^{-1}$ ,  $e_{\pi c} = 780 \text{ cm}^{-1}$  and finally, for a test of the formulas used, to  $Dq = 1860 \text{ cm}^{-1}$ .

The corresponding procedure carried out for the  $\text{Cr}(\text{acac})_3$  complex yields  $\alpha = 93.2$ ,  $e_{\pi s} = 1060 \text{ cm}^{-1}$ ,  $e_\sigma = 7180 \text{ cm}^{-1}$  and  $Dq = 1840 \text{ cm}^{-1}$ . These numbers are well within the trends expected from a comparison of AOM parameters of different central metal ions, *i.e.* the  $\pi$ -metal–ligand interaction  $e_{\pi s}$  for Co is larger than for Cr, while values of ligand field parameter  $Dq$  for these ions are more similar to one another.

For a more accurate calculation the non-diagonal matrix elements of  $t_{2g}$  with  $e_g$ -orbitals in Table II must be considered. Although  $e_\sigma$ -parameters are usually large, these matrix elements are nevertheless small for bite angles close to  $90^\circ$  due to the cosine factor. Characteristic values for these matrix elements are  $300\text{--}600 \text{ cm}^{-1}$  which are small compared to  $10Dq = 18000 \text{ cm}^{-1}$  by which the unperturbed  $t_{2g}$ - and  $e_g$ -orbitals at cubic symmetry are separated. The changes obtained from a consideration of non-diagonal matrix elements are therefore expected to be relatively small. As an example calculations have been carried out with the full orbital perturbation matrix using appropriate AOM and Racah parameters. The results obtained as a consequence of configuration interaction indicate slight decreases ( $\sim 50 \text{ cm}^{-1}$ ) of trigonal orbital splittings (compared to a total of  $\sim 1500 \text{ cm}^{-1}$ ) and small changes ( $\sim 1^\circ$ ) of the bite angle  $\alpha$ . These can, however, be neglected in view of the fact that other interactions, as for example lattice effects and restoring forces which have not been included in the present model, are expected to con-

tribute to the results by the same order of magnitude. They may become, however, important for larger changes of bite angle  $\alpha$ . The inclusion of  $e_g$  orbital mixing, in any case, tends to increase the bite angle by a limited amount as is also the case for occupation of these orbitals in high spin complexes such as Mn(III) and Fe(III) (see above).

### Jahn–Teller Effects in the Excited State

In addition to phase coupling effects the ground state geometry and the low symmetry level splittings may also be explained by the operation of Jahn–Teller forces. These can be effective either by  $e_g$  or  $\tau_{2g}$  active vibration leading to tetragonal, orthorhombic or trigonal distortions. In  $\text{Mn}(\text{acac})_3$  the ligand field of trigonally arranged acetylacetonate ligands is superimposed by a tetragonal component due to the Jahn–Teller effect in the ground state [12, 23]. Jahn–Teller activity by  $e_g$  vibrational modes in the  ${}^4T_{2g}$  excited state leading to a splitting of  $310 \text{ cm}^{-1}$  has been observed, *e.g.*, in  $\text{CrCl}_6^{3-}$  doped in the In(III) elpasolite [26]. For  $\text{Cr}(\text{acac})_3$  a  $T_2 \otimes e$  Jahn–Teller effect in this excited state is, however, very improbable. The reasoning for this is based on the results obtained from the polarized spectra of the optically uni-axial crystals which exhibit equal intensity relations for the  $\alpha$  and  $\sigma$  spectrum, *i.e.*  $\alpha = \sigma \neq \pi$  characteristic for electric dipole transitions [17]. If a  $C_4$  axis would be superimposed on the trigonal complex chromophores the extinction of the  $\alpha$ -spectrum is  $\phi$ -dependent where  $\phi$  denotes the angle between the electric dipole vector  $\vec{E}$  and the projection of the  $C_4$  axis in the  $x, y$  plane. Since the  $\alpha$ -spectrum is measured to be independent of  $\phi$  (own results), a  $T_2 \otimes e$  Jahn–Teller effect can be excluded because of different tetragonal selection rules operative for transitions into  ${}^4B_{2g}$  (only  $\sigma$ -polarized) and  ${}^4E_g$  ( $\sigma$ - and  $\pi$ -polarized). If there is an equally distributed distortion by induction of  $C_4$  axes in the lattice forming crystal domains no polarization due to the Jahn–Teller effect would be obtained. A statistically distributed distortion in any case will contribute to splittings of unpolarized absorption bands. The measured band splittings in the polarized spectrum indicating large contributions due to the static trigonal field may therefore have small components of unpolarized absorptions arising from pseudo-isotropic Jahn–Teller distortions. Equal polarizations, similar relation intensities and splittings of the first allowed bands measured for the Cr- and Co-trisacetylacetonate spectra, however, do not support the presence of a tetragonal Jahn–Teller effect. Different geometries of these compounds should give rise to remarkable differences in the spectra.

The Jahn–Teller effect due to  $\tau_2$  vibrational activity on the other hand is usually much smaller. It

can, however, be present and may contribute to the observed splitting of the first spin-allowed transitions arising from the trigonal ligand field in Cr- and Co-trisacetylacetonates. A calculation of vibronic  $T \otimes \tau_2$  coupling performed with the first order perturbation matrix [27] yields for the observed level sequence  $A < E$  bite angles of  $\alpha < 90^\circ$ , i.e. a squeezing of the complex octahedron along the trigonal axes which proceeds into the opposite direction to the X-ray structural results (cf. Table I). From the calculated vibronic coupling coefficients  $f_T$  and appropriate force constants  $k_T$  for the  $\tau_2$  vibration a Jahn–Teller stabilization energy  $E_{JT} = (\frac{2}{3})f_T^2/k_T$  of only 10–20  $\text{cm}^{-1}$  is calculated. We can conclude that, as far as the splittings of the excited T states are concerned, the Jahn–Teller activity due to  $\tau_2$  active vibrations is very small, the distortion leading in the opposite direction compared to what is obtained from orbital phase coupling effects. Also, since the Jahn–Teller forces are small not much influence is expected on the geometry of the ground state by virtue of second order effects. For  $\text{Co}(\text{acac})_3$  exhibiting the largest distortion from octahedral symmetry this Jahn–Teller effect can be excluded since coupling of  ${}^1A_{1g}$  ground state with first excited  ${}^1T_{1g}$  is not possible by Jahn–Teller active modes due to symmetry reasons. If any Jahn–Teller activities are present they would be dominated by phase coupling effects which, for reasonable sets of AOM parameters, are large enough for explaining ground state geometries and correct level splittings in the excited state.

## References

- 1 E. C. Lingafelter and R. L. Braun, *J. Am. Chem. Soc.*, **88**, 2951 (1966).
- 2 D. L. Kepert, *Inorg. Chem.*, **11**, 1561 (1976).
- 3 P. O. Hon and C. E. Pfluger, *J. Coord. Chem.*, **3**, 67 (1973).
- 4 A. Avdeef and J. P. Fackler, Jr., *Inorg. Chem.*, **14**, 2002 (1975).
- 5 G. St. Nikolov and N. Trendafilova, *Inorg. Chim. Acta*, **68**, 29 (1983).
- 6 C. E. Pfluger and P. S. Haradem, *Inorg. Chim. Acta*, **69**, 141 (1983).
- 7 G. Kung-Jon Chao, R. Lewin Sime and R. J. Sime, *Acta Crystallogr., Sect. B*, **29**, 2845 (1973).
- 8 K. Dymock and G. J. Palenik, *Acta Crystallogr., Sect. B*, **30**, 1364 (1974).
- 9 T. J. Anderson, M. A. Neuman and G. A. Melson, *Inorg. Chem.*, **12**, 927 (1973).
- 10 B. Morosin and H. Montgomery, *Acta Crystallogr., Sect. B*, **25**, 1354 (1969).
- 11 B. Morosin, *Acta Crystallogr., Sect. B*, **19**, 131 (1965).
- 12 J. P. Fackler and A. Avdeef, *Inorg. Chem.*, **13**, 1864 (1974).
- 13 J. Iball and C. H. Morgan, *Acta Crystallogr., Sect. B*, **23**, 239 (1967).
- 14 C. J. Kruger and E. C. Reynhardt, *Acta Crystallogr., Sect. B*, **30**, 822 (1974).
- 15 L. E. Orgel, *J. Chem. Soc.*, 3683 (1961).
- 16 A. Ceulemans, M. Dendooven and L. G. Vanquickenborne, *Inorg. Chem.*, **24**, 1153 (1985).
- 17 M. A. Atanasov, T. Schönherr and H.-H. Schmidtke, *Theor. Chim. Acta*, **71**, 59 (1987).
- 18 S. Sugano, Y. Tanabe and H. Kamimura, 'Multiplets of Transition Metal Ions in Crystals', Academic Press, New York, 1970.
- 19 T. S. Piper, *J. Chem. Phys.*, **35**, 1240 (1961).
- 20 T. S. Piper and R. L. Carlin, *J. Chem. Phys.*, **36**, 3330 (1962).
- 21 N. C. Moucharafieh, P. G. Eller, J. A. Bertrand and D. J. Royer, *Inorg. Chem.*, **17**, 1220 (1978).
- 22 R. D. Peacock, *J. Chem. Soc., Dalton Trans.*, 291 (1983).
- 23 R. Dingle, *J. Mol. Spectrosc.*, **9**, 426 (1962).
- 24 C. K. Jørgensen, 'Absorption Spectra and Chemical Bonding in Complexes', Pergamon, Oxford, 1962.
- 25 M. A. Atanasov and G. St. Nikolov, *Comm. Dep. Chem. Bulg. Acad. Sci.*, **16**, 329 (1983).
- 26 H. U. Güdel and T. R. Snellgrove, *Inorg. Chem.*, **17**, 1617 (1978).
- 27 I. B. Bersuker, 'The Jahn–Teller Effect and Vibronic Interaction in Modern Chemistry', Plenum Press, New York, 1984.